

Linköping University Post Print

Magic and hot giant fullerenes formed inside ion irradiated weakly bound C-60 clusters

H Zettergren, H A B Johansson, H T Schmidt, Jens Jensen, P Hvelplund, S Tomita, Y Wang, F Martin, M Alcamí, B Manil, L Maunoury, B A Huber and H Cederquist

N.B.: When citing this work, cite the original article.

Original Publication:

H Zettergren, H A B Johansson, H T Schmidt, Jens Jensen, P Hvelplund, S Tomita, Y Wang, F Martin, M Alcamí, B Manil, L Maunoury, B A Huber and H Cederquist, Magic and hot giant fullerenes formed inside ion irradiated weakly bound C-60 clusters, 2010, JOURNAL OF CHEMICAL PHYSICS, (133), 10, 104301.

<http://dx.doi.org/10.1063/1.3479584>

Copyright: American Institute of Physics

<http://www.aip.org/>

Postprint available at: Linköping University Electronic Press

<http://urn.kb.se/resolve?urn=urn:nbn:se:liu:diva-60701>

Magic and hot giant fullerenes formed inside ion irradiated weakly bound C₆₀ clusters

H. Zettergren,^{1,a)} H. A. B. Johansson,¹ H. T. Schmidt,¹ J. Jensen,² P. Hvelplund,³ S. Tomita,⁴ Y. Wang,⁵ F. Martín,⁵ M. Alcamí,⁵ B. Manil,⁶ L. Maunoury,⁷ B. A. Huber,⁷ and H. Cederquist¹

¹Department of Physics, Stockholm University, SE-106 91 Stockholm, Sweden

²Department of Physics, Chemistry and Biology (IFM), Linköping University, SE-581 83 Linköping, Sweden

³Department of Physics and Astronomy, Aarhus University, DK-8000 Aarhus C, Denmark

⁴Institute of Applied Physics, University of Tsukuba, Tsukuba, Ibaraki 305-0006, Japan

⁵Departamento de Química, C-9, Universidad Autónoma de Madrid, 28049 Madrid, Spain

⁶Laboratoire de Physique des Lasers (LPL) UMR 7538 CNRS, Institut Galilée, Université Paris 13,

Av. J.B. Clément F-93430 Villetaneuse, France

⁷Centre de Recherche sur les Ions, les Matériaux et la Photonique (CIMAP), Bd Henry Becquerel, F-14070 Caen Cedex 05, France

(Received 3 June 2010; accepted 25 July 2010; published online 9 September 2010)

We find that the most stable fullerene isomers, C₇₀–C₉₄, form efficiently in close-to central collisions between keV atomic ions and weakly bound clusters of more than 15 C₆₀-molecules. We observe extraordinarily high yields of C₇₀ and marked preferences for C₇₈ and C₈₄. Larger even-size carbon molecules, C₉₆–C₁₈₀, follow a smooth log-normal (statistical) intensity distribution. Measurements of kinetic energies indicate that C₇₀–C₉₄ mainly are formed by coalescence reactions between small carbon molecules and C₆₀, while C_n with $n \geq 96$ are due to self-assembly (of small molecules) and shrinking hot giant fullerenes. © 2010 American Institute of Physics.

[doi:10.1063/1.3479584]

I. INTRODUCTION

The discoveries of fullerenes in 1985,¹ carbon nanotubes in 1991,² and the large-scale productions of these species in the 1990s (Ref. 3) paved the road to fullerene science. Due to their extraordinary structural properties in which all 12 pentagonal faces are isolated on the closed caged surfaces, C₆₀ and C₇₀ are more stable than their nearest neighbor fullerenes. However, the binding energy per atom increases with fullerene size⁴ and it is thermodynamically more preferable to form even larger fullerenes. Thus, much work has been devoted to attempts to understand the well-established preferences for forming C₆₀ and C₇₀ in a large variety of experimental, industrial, and naturally occurring situations including laser ablations of graphite^{1,5}—and virtually of any carbon-based material, arc discharges between graphite rods,³ sooting flames,⁶ large-scale industrial combustion,⁷ and when burning a candle.⁸ Recently Irle *et al.* presented quantum chemical molecular dynamics simulations suggesting that hot giant fullerenes, C_n with $n > \sim 90$, self-assemble in hot carbon and hydrocarbon vapors.^{9,10} In these calculations, the hot giant fullerenes (vibrationally highly excited and with distorted structures) shrink spontaneously to smaller fullerenes—mostly by C₂-emissions far from thermal equilibrium. It is envisaged that C₆₀ and C₇₀ then will form with high probabilities.^{9,10} This combination of size-up and long-range, multistep, size-down fullerene formation is clearly different from earlier models in which C₆₀ and C₇₀

are assumed to be formed through size-up processes followed by fragmentation in few steps only. Here, we will discuss such formation scenarios—and various types of coalescence reactions in view of the intensities and kinetic energies of even- n C₇₀⁺–C₁₈₀⁺ ions which we measure following 400 keV head-on Xe²⁰⁺ collisions with weakly bound [C₆₀]_m clusters.

Coalescence reactions involving fullerenes have been observed before in, e.g., fullerene-fullerene collisions,¹¹ laser desorptions of fullerene films,^{12,13} and femtosecond laser pulse interactions with weakly bound [C₆₀]_m clusters.¹⁴ Here we will demonstrate that ion impact on such [C₆₀]_m clusters induces different kinds of molecular fusion reactions as the energy [typically hundreds of eV per C₆₀ molecule on the ion trajectory for 400 keV Xe²⁰⁺ (Ref. 15)] is deposited much more locally than with laser excitations.

II. EXPERIMENT

The experiment was performed at the ARIBE facility, Caen, France, with a pulsed 400 keV Xe²⁰⁺-beam crossing [C₆₀]_m target jets. Ions formed in the collisions (clusters, monomers, and fragments) were analyzed with a linear time-of-flight spectrometer. The [C₆₀]_m targets were produced by letting initially hot C₆₀ monomers (from a temperature regulated oven) interact with He gas at 77 K. This method only allows fullerene-fullerene collisions at very low relative energies and with internally cold fullerenes such that only weak, van der Waals type, C₆₀–C₆₀ bonds may form. Formations of single covalent bonds have a prohibitively high reaction barrier of 1.6 eV (Ref. 16) while C₁₂₀ formation re-

^{a)}Author to whom correspondence should be addressed. Electronic mail: henning@fysik.su.se.

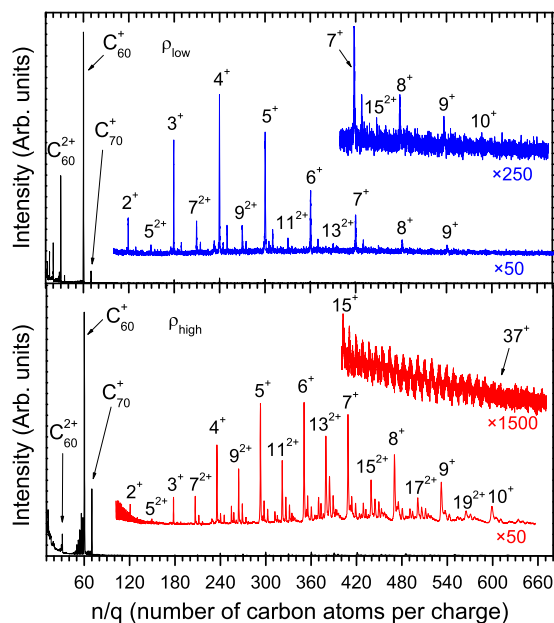


FIG. 1. Size distributions of clusters of fullerenes recorded with low (ρ_{low} , upper panel) and high (ρ_{high} , lower panel) fullerene monomer densities in the cluster source (cf. text). The $[\text{C}_{60}]_m^+$ and $[\text{C}_{60}]_m^{2+}$ peaks are denoted by m^+ and m^{2+} . The ($\times 1500$)-inset starts at $n/q=890$.

quires 80–85 eV collision energies.¹⁷ We operate the cluster source in two modes with low fullerene monomer density (ρ_{low}), obtained with an oven temperature $T=530^\circ\text{C}$ and high density (ρ_{high}) with $T=590^\circ\text{C}$.

III. RESULTS AND DISCUSSION

Part of the results is shown in Fig. 1 where we see a shift toward larger cluster sizes for ρ_{high} . Zoom-ins reveal that the $[\text{C}_{60}]_m$ -distributions range up to $m \sim 15$ and $m \sim 40$ for ρ_{low} and ρ_{high} , respectively. Note also the increased intensities (and shifts toward larger masses) for the smaller peaks between the $[\text{C}_{60}]_m^+$ -peaks for ρ_{high} in comparison with ρ_{low} . These smaller peaks are mainly due to larger- m , multiply charged intact clusters of fullerenes. In the ρ_{low} case, the $n/q=60$ peak is mainly due to single ionization of C_{60} monomers in the target. Likewise, the intensity of the C_{70}^+ peak is dominated by single ionizations of C_{70} monomers—there is 4% C_{70} and 96% C_{60} in the fullerene powder—and for ρ_{low} we indeed measure the C_{70}^+ intensity to be close to 4% of that for C_{60}^+ . However, as seen in Fig. 1 the $\text{C}_{70}^+/\text{C}_{60}^+$ ratio is much higher for ρ_{high} . Indeed, even when we include the intensities in the C_2 -evaporation series of C_{60}^+ , the intensity ratio $I(\text{C}_{70}^+)/\sum_k I(\text{C}_{60-2k}^+)$ ($k=0,1,\dots$) is found to increase from 0.045 ± 0.001 for ρ_{low} —consistent with the powder mixture—to 0.084 ± 0.003 for ρ_{high} . Thus, at least $46 \pm 2\%$ of the C_{70}^+ intensity for ρ_{high} is due to C_{70} -formation catalyzed by Xe^{20+} impact, while the remaining part is due to single ionizations of C_{70} monomers and intact C_{70}^+ emitted from ionized mixed $[(\text{C}_{60})_m-(\text{C}_{70})_l]$ clusters [C_{70} clusters in the same way as C_{60} (Refs. 18 and 19) and the present intensity distributions as functions of l for given m are indeed given by the 4% C_{70} content in the powder at ρ_{low} and ρ_{high}].

A zoom-in on the $n/q \leq 180$ region is shown in Fig. 2. The C_2 -evaporation series to the left of the C_{60}^+ peak is due to

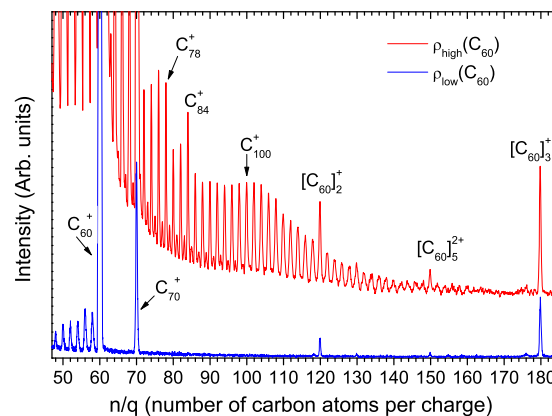


FIG. 2. Intensities due to $\text{Xe}^{20+} + [\text{C}_{60}]_m$ collisions for ρ_{low} (below) and ρ_{high} (above). Fullerene dimers, trimers, and pentamers are indicated with $[\text{C}_{60}]_2^+$, $[\text{C}_{60}]_3^+$, and $[\text{C}_{60}]_5^{2+}$ and fullerene monomers with C_n^+ (cf. text).

highly excited C_{60}^+ , emitted from multiply ionized $[\text{C}_{60}]_m$ clusters, which later (as they are hot) emit one or several C_2 units.²⁰ A key aspect here is that (charged) clusters of fullerenes, in contrast to, e.g., weakly bound argon clusters,²¹ are excellent electrical conductors²⁰ within which the charge is distributed on subfemtosecond time scales.^{22,23} Thus, a Xe^{20+} ion may, e.g., pass closely outside a $[\text{C}_{60}]_m$ surface and initially removes many electrons from individual C_{60} molecules and then also excites them strongly. These charges spread out before the C_{60}^+ are emitted from the cluster (picosecond timescales) and these fullerenes may also fragment but on even longer time scales (nano- to microseconds typically). For ρ_{high} a broad intensity distribution with peaks separated by two carbon masses appears with very small odd (n/q)-peaks in between. As this distribution is absent for ρ_{low} there is a clear correlation between large clusters ($m > 15$) in the target and C_n^+ production, showing that these molecules mainly form *inside* the $[\text{C}_{60}]_{m \geq 15}$ -clusters and not on their surfaces. In the latter case we would observe this distribution—or at least traces of it—also for ρ_{low} .

In Fig. 3, we show integrated $\text{C}_{n \geq 70}^+$ intensities (from Gaussian fits) after subtracting the background tail from the C_{60}^+ peak (cf. Fig. 2) and the C_{70}^+ contribution due to the 4% C_{70} -content in the powder. The remaining C_{70}^+ intensity is responsible for $56 \pm 4\%$ of all $\text{C}_{n \geq 70}^+$ fullerenes formed. In femtosecond laser excitation of $[\text{C}_{60}]_m$ (Ref. 14) and in laser desorptions of C_{60} -films¹² there are broad maxima around $n=120, 180, 240$, etc., indicating that the fused fullerenes in these experiments are due to coalescence reactions involving two, three, four, etc., fullerene monomers. In the present case, the C_n^+ distribution is markedly different with a broad maximum (peaking well below $n=120$ but also extending rather far beyond this value) and, notably, with a strongly structured distribution in the C_{70} – C_{96} region. For $n \geq 96$ our distribution fits nicely to a log-normal function $f_{N,\sigma}(n) \propto (2\pi n^2 \sigma^2)^{-1/2} \exp[-(\ln(n/N))^2 / (2\sigma^2)]$ with a mean value $N=103.5$ and shape parameter $\sigma=0.1$.²⁴ This strongly indicates a statistical growth to a hot giant fullerene distribution very much like the ones obtained with laser ablation of $\text{C}_7\text{H}_6\text{O}_4$.²⁴ In contrast, the C_{70} – C_{96} region exhibits large peak variations and, thus, their formation mechanisms are most likely different. A picture including size-up processes from

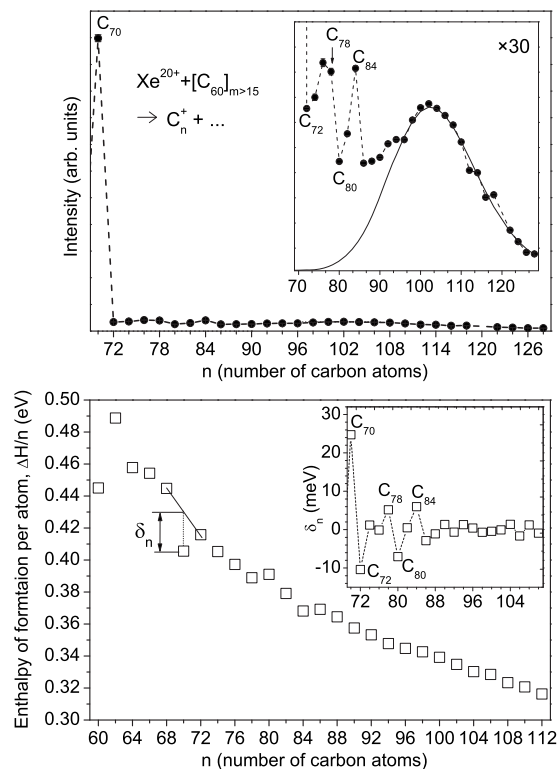


FIG. 3. Upper panel: measured C_n^+ -intensities due to 400 keV $Xe^{20+} + [C_{60}]_{m>15}$ collisions as a function of n . The solid curve in the inset is a log-normal fit for $n \geq 96$. Error bars are smaller than the symbols. Lower panel: calculated enthalpies of formation per carbon atom for the lowest energy isomers of C_n fullerenes. Inset: the mean nearest neighbor enthalpy difference δ_n (cf. text).

C_{60} appears reasonable and is consistent with interpretations of experiments on laser desorption of surfaces covered with C_{60} ,²⁵ in which fused fullerenes—with a similar intensity distribution in the $n=72$ – 84 range as the present one—were recorded with such low laser fluence that only very few fullerenes beyond C_{84} were produced. This distribution was interpreted as being due to C_{60} size-up processes involving absorption of smaller carbon molecules from nearby fragmented fullerenes. At higher laser fluence,²⁵ a smooth distribution of larger fullerenes appeared and was ascribed to self-assembly of small carbon molecules. In the present experiment, and in Ref. 26, the C_{60}^+ peaks have tails toward larger masses (cf. Fig. 2) which are signatures of size-up processes to C_{60+2k}^+ ($k > 0$) and fragmentation in the spectrometer extraction field.²⁶

To further aid the interpretation of the results, we have performed high level density functional theory calculations (B3LYP/6-31G* level of theory)²⁷ for the most stable C_{60} – C_{112} fullerene isomers (thus extending the results in relation to Ref. 28). Calculated structures have been fully optimized without any symmetry constraint and the related enthalpies of formation per carbon atom [$\Delta H(n)/n$] as functions of C_n^+ size are shown in Fig. 3. These follow a smooth decreasing trend for $n > 90$ and approach zero as $n \rightarrow \infty$ [here zero is the $\Delta H(n)/n$ -value for graphite which corresponds to the largest binding energy per atom]. As a measure of the C_n stability, we define the mean nearest neighbor enthalpy difference, $\delta_n = 0.5(\Delta H(n-2)/(n-2)$

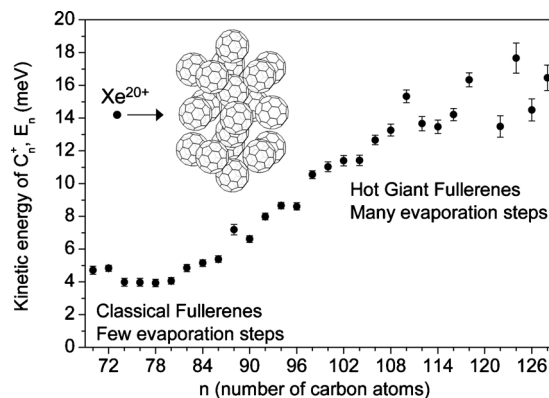


FIG. 4. Kinetic energies of C_n^+ ions as a function of size n .

$+\Delta H(n+2)/(n+2) - \Delta H(n)/n$, which is positive (negative) for a minimum (maximum) in the enthalpy sequence and thus a positive δ_n should correspond to a magic C_n fullerene (lower inset in Fig. 3). The correlation between the δ_n -sequence and the measured C_n^+ intensities is striking with maxima (minima) for $n=70, 78, 84$ ($n=72, 80$) in agreement with the expected sizes for magic (nonmagic) fullerenes and we thus conclude that the lowest energy C_n isomers—or isomers almost degenerate in energy with the most stable ones—form in this n -region.

In Fig. 4, we show measurements of mean C_n^+ kinetic energies. These are extracted as $E_n = \Delta t^2 \epsilon^2 / (8\mu)$,²⁹ where μ is the C_n^+ mass, Δt is the peak width in the time-of-flight spectrum after deconvolution with the instrumental width, and $\epsilon = 77.1$ V/cm is the extraction field strength. For molecular decay processes yielding two fragments there is a simple relation between the total kinetic energy—the kinetic energy release (E_{KER})—and the kinetic energy for one fragment. In the case of $C_{n+2}^+ \rightarrow C_n^+ + C_2$, $E_{KER} = (n/2 + 1)T_n$ where T_n is the final kinetic energy of C_n^+ . Normally E_{KER} is quite small when a single neutral C_2 molecule is emitted from a C_n^+ fullerene and a typical value is $E_{KER} = 150$ meV.^{30,31} For a one-step fragmentation process such as $C_{72}^+ \rightarrow C_{70}^+ + C_2$ this gives $T_{70} = E_{70} = 4.2$ meV while, e.g., two or five steps of sequential C_2 -emission from C_{74}^+ and C_{80}^+ would give $E_{70} = 8.2$ meV and 19.8 meV, respectively. The measured E_n -values for C_{70} – C_{86} are only 4–5 meV and thus far too small for any charge separation process (as, e.g., C_2 -emission) or for longer sequences of neutral C_2 emissions.^{30,31} Instead, it appears that these fullerenes form through size-up processes and fragmentation in few steps only. Above C_{86} , the E_n -values increase with n . As an example $E_{128} = 16.5 \pm 0.8$ meV, which allows for about seven $E_{KER} = 150$ meV C_2 -emissions.^{30,31}

We have already concluded that the new larger C_n^+ fullerenes only are formed with sufficiently large $[C_{60}]_m$ clusters in the target and it appears that both the magic fullerenes and the hot giant fullerenes are formed in $[C_{60}]_m$ bulks. There, C_{60} molecules near central trajectories (cf. inset of Fig. 4) are shattered in small fragments while those about a C_{60} radius away may remain intact or almost intact. Thus, the hot giant fullerenes may be self-assembled from the carbon plasma while the magic fullerenes could be formed in

coalescence reactions between small (e.g., C_2) molecules from the plasma and surrounding, essentially undamaged, fullerenes.

IV. CONCLUSION

In this paper, we have shown that the C_{70} – C_{86} and $C_{n>90}$ fullerenes may be due to very different types of formation processes. In the former case the lowest energy fullerene isomers appear to form efficiently through coalescence reactions in which smaller carbon molecules, such as C_2 , are absorbed by C_{60} -fullerenes in $[C_{60}]_m$ clusters. Measured C_n^+ kinetic energies strongly indicate that at most a few fragmentation steps are needed to cool these systems such that they become stable on the experimental time scale of tens of microseconds. This is also consistent with the highly efficient production of the magic fullerenes C_{78} and C_{84} , and, in particular, C_{70} (more than 30 times more C_{70} than C_{72} is formed), which requires formation processes very sensitive to local variations in the C_n enthalpies of formation. Above C_{90} , in contrast, the recorded lognormal intensity distribution and the much larger C_n^+ kinetic energies suggest statistical growth (self-assembly) processes all the way from small carbon molecules to hot giant fullerenes followed by sequential emission processes in many steps. Thus, hot shrinking giant fullerenes cannot be involved in the main route to C_{70} formation—at least not under the present experimental conditions. Instead it appears that the production of smaller and somewhat colder fullerenes slightly above C_{70} (like for the present coalescence reactions) strongly favors efficient production of magic C_{70} .

ACKNOWLEDGMENTS

The Swedish Research Council, the ITS-LEIF Project (No. RII3-026015), and the Spanish DGI Project Nos. FIS 2007-60064 and CSD 2007-00010 are gratefully acknowledged. We thank the CCC-UAM and BSC for computer time.

¹H. W. Kroto, J. R. Heath, S. C. O'Brien, R. F. Curl, and R. E. Smalley, *Nature (London)* **318**, 162 (1985).

²S. Iijima, *Nature (London)* **354**, 56 (1991).

³W. Krätschmer, L. D. Lamb, K. Fostiropoulos, and D. R. Huffman, *Nature (London)* **347**, 354 (1990).

⁴B. I. Dunlap, *Int. J. Quantum Chem.* **64**, 193 (1997).

⁵Z.-X. Xie, Z.-Y. Liu, C.-R. Wang, R.-B. Huang, F.-C. Lin, and L.-S. Zheng, *J. Chem. Soc., Faraday Trans.* **91**, 987 (1995).

⁶J. B. Howard, J. T. McKinnon, A. L. L. Y. Makarovskiy, and M. E.

Johnson, *Nature (London)* **352**, 139 (1991).

⁷See: <http://www.nano-c.com/index.html> for an example of combustion-based process technology.

⁸P. Gerhardt, S. Löffler, and K. H. Homann, *Chem. Phys. Lett.* **137**, 306 (1987).

⁹S. Irle, G. Zheng, and K. Morokuma, *J. Phys. Chem. B* **110**, 14531 (2006).

¹⁰B. Saha, S. Shindo, S. Irle, and K. Morokuma, *ACS Nano* **3**, 2241 (2009).

¹¹F. Rohmund, E. E. B. Campbell, O. Knospe, G. Seifert, and R. Schmidt, *Phys. Rev. Lett.* **76**, 3289 (1996).

¹²C. Yeretizian, K. Hansen, F. Diederich, and R. L. Whetten, *Nature (London)* **359**, 44 (1992).

¹³R. Mitzner, B. Winter, C. Kusch, E. Campbell, and I. Hertel, *Z. Phys. D: At., Mol. Clusters* **37**, 89 (1996).

¹⁴M. Hedén, K. Hansen, and E. E. B. Campbell, *Phys. Rev. A* **71**, 055201 (2005).

¹⁵S. Martin, R. Bredy, J. Bernard, L. Chen, M. C. Buchet-Poulizac, and A. Salmoun, *Nucl. Instrum. Methods Phys. Res. B* **209**, 265 (2003).

¹⁶D. Porezag, M. R. Pederson, T. Frauenheim, and T. Köhler, *Phys. Rev. B* **52**, 14963 (1995).

¹⁷E. E. Campbell, *Fullerene Collision Reactions*, 1st ed. (Kluwer Academic, Dordrecht, 2003).

¹⁸K. Hansen, R. Müller, H. Hohmann, and E. E. B. Campbell, *Z. Phys. D* **40**, 361 (1997).

¹⁹H. Zettergren, H. T. Schmidt, P. Reinhed, H. Cederquist, J. Jensen, P. Hvelplund, S. Tomita, B. Manil, J. Rangama, and B. A. Huber, *J. Chem. Phys.* **126**, 224303 (2007).

²⁰B. Manil, L. Maunoury, B. A. Huber, J. Jensen, H. T. Schmidt, H. Zettergren, H. Cederquist, S. Tomita, and P. Hvelplund, *Phys. Rev. Lett.* **91**, 215504 (2003).

²¹W. Tappe, R. Flesch, E. Rühl, R. Hoekstra, and T. Schlathöler, *Phys. Rev. Lett.* **88**, 143401 (2002).

²²H. Zettergren, H. T. Schmidt, P. Reinhed, H. Cederquist, J. Jensen, P. Hvelplund, S. Tomita, B. Manil, J. Rangama, and B. A. Huber, *Phys. Rev. A* **75**, 051201 (2007).

²³H. Zettergren, Y. Wang, A. M. Lamsabhi, M. Alcamí, and F. Martín, *J. Chem. Phys.* **130**, 224302 (2009).

²⁴J. Maul, T. Berg, E. Marosits, G. Schönhense, and G. Huber, *Phys. Rev. B* **74**, 161406 (2006).

²⁵G. Ulmer, E. E. B. Campbell, R. Kühnle, H. G. Busmann, and I. V. Hertel, *Chem. Phys. Lett.* **182**, 114 (1991).

²⁶M. F. Budyka, T. S. Zyubina, A. G. Ryabenko, E. Muradyan, S. E. Esipov, and N. I. Cherepanova, *Chem. Phys. Lett.* **354**, 93 (2002).

²⁷M. J. Frisch, G. W. Trucks, H. B. Schlegel *et al.*, GAUSSIAN 03, Revision B.03, Gaussian, Inc., Wallingford, CT, 2004.

²⁸J. Cioslowski, N. Rao, and D. Moncrieff, *J. Am. Chem. Soc.* **122**, 8265 (2000).

²⁹S. Tomita, H. Lebius, A. Brenac, F. Chandezon, and B. A. Huber, *Phys. Rev. A* **67**, 063204 (2003).

³⁰K. Gluch, S. Matt-Leubner, O. Echt, B. Concina, P. Scheier, and T. D. Märk, *J. Chem. Phys.* **121**, 2137 (2004).

³¹N. Haag, Z. Berényi, P. Reinhed, D. Fischer, M. Gudmundsson, H. A. B. Johansson, H. T. Schmidt, H. Cederquist, and H. Zettergren, *Phys. Rev. A* **78**, 043201 (2008).